Neural, Parallel, and Scientific Computations 25 (2017) 457-468

SUPER TIME-STEPPING SCHEMES FOR CONDUCTION-RADIATION HEAT TRANSFER PROBLEM

PINEYRO BENEDICT[1] AND HARIHAR KHANAL[1]

[1]Department of Mathematics, Embry-Riddle Aeronautical University,
Daytona Beach, FL 32114-3900, U.S.A.

ABSTRACT. We solve a nonlinear parabolic partial differential equation describing conduction-radiation heat transfer in a semitransparent medium (glass) numerically using an explicit finite volume method. To overcome the stability restriction of the explicit method we employ two first order super time-stepping (STS) schemes based on Chebyshev and Legendre polynomials and compare their performances.

Key Words: conduction-radiation, diffusion approximation, super time-stepping schemes

AMS (MOS) Subject Classification. 35Q35, 45K05, 65Z05.

1. Introduction

In many industrial processes, temperature is generally very high resulting in a strong contribution from the radiative transfer to the overall transport of energy within the system. Conduction-radiation heat transfer problems are usually formulated with highly nonlinear integro-differential equations. Using the diffusion approximation to the radiation transfer equation, the model can be reduced to a nonlinear parabolic partial differential equations [3]. An excellent survey on radiation transfer in participating media with major events in the development of engineering treatment can be found in [5]. Since the coupling between the energy equation and the equation of radiative transfer is highly nonlinear, it is of utmost importance to utilize efficient and accurate solution procedures. Explicit schemes are simple and accurate to implement and convenient for parallelization but suffer severely with stability restriction on the time step-size. On the other hand, implicit schemes involve iterative approach to solve the nonlinear systems, hence are moderately efficient, can be computationally very costly for highly nonlinear problems, and comparatively difficult to implement in practice specially for the problems with intricate geometry. Due to its popularity (easy to parallelize for high performance computing), there has been some efforts expended in developing super time-stepping (STS) strategies to overcome the stability restriction of the explicit schemes [1, 4]. The STS schemes can be viewed as

Received April 15, 2017

the stabilized Runge-Kutta (RK) methods where the updates in the internal stages s are strategically devised to fulfill the stability condition in contrast to improve the accuracy or order of the scheme in the standard RK family.

In this paper, we implement two first order STS schemes based on Chebysheb polynomial (RKC) [1] and Legendre polynomial (RKL) [5] on the finite volume code for combined conduction radiation transfer in a semitransparent material (glass). The numerical simulations show that both the STS schemes (RKC and RKL) agree well and boast large efficiency gains compared to standard explicit methods.

The rest of the paper is organized as follows. Section §2 describes briefly a mathematical model for conduction-radiation transfer in semitransparent medium with an arbitrary varying spectral absorption coefficient. Numerical schemes based on explicit finite volume approximation to the partial differential equation employing two STS strategies are developed in section §3. Some numerical simulation results are presented in §4, with conclusions in §5.

2. **Mathematical Model**

Here we describe a simple model for conduction-radiation heat transfer problem based on Rosseland approximation [3]. The equation for conservation of energy for conduction-radiation heat transfer problem in one dimension has the form

$$\rho C(T)\frac{\partial T}{\partial t} = \frac{\partial}{\partial z}\left(K_c(T)\frac{\partial T}{\partial z} - Q\right),\ 0 < z < l, \tag{2.1}$$

where ρ is the density of the material, $C(T)$ is the specific heat capacity of the medium, $K_c(T)$ is the thermal conductivity, Q is the radiation heat flux.

The radiation heat flux Q is obtained by integrating the radiation intensity which is described by a highly nonlinear integro-differential equation. Using Rosseland approximation to the radiative transfer equation, which is valid for optically thick medium, the radiative heat flux can be expressed as [5]

$$Q = -\frac{4\pi}{3a(\nu)}\frac{\partial I_b(\nu, T)}{\partial T}\frac{\partial T}{\partial z}. \tag{2.2}$$

Here $a(\nu)$ is the spectral absorption coefficient, ν is the wavelength and I_b is the spectral intensity of black body radiation given by the Planck function

$$I_b(\nu, T) = \frac{2h_p\nu^3}{c_g^2\left(\exp\left(\frac{h_p\nu}{k_bT} - 1\right)\right)}. \tag{2.3}$$

with c_g is the speed of propagation of light in the medium, h_p is Plank's constant and k_b is Boltzmann's constant.

Adopting a multi-band model for absorption coefficient $a(\nu)$, we approximate the spectral absorption coefficient in each of the frequency band $\nu_k \leq \nu \leq \nu_{k+1}$ by

a piecewise constant function $a(\nu)$. For $\nu \in [\nu_k, \nu_{k+1})$, we define $a_k := a(\nu) = a(\nu_k)$ and $I_b^{(k)}(T) := \int_{v_k}^{v_{k+1}} I_b(\nu, T)d\nu$. Thus, equation (2.1) takes the form

$$\rho C(T)\frac{\partial T}{\partial t} = \frac{\partial}{\partial z}\left(K(T)\frac{\partial T}{\partial z}\right),\ 0 < z < l, \tag{2.4}$$

where

$$K(T) = K_c(T) + \sum_k^{M_k} \frac{4\pi}{3a_k}\frac{\partial I_b^{(k)}}{\partial T}. \tag{2.5}$$

Considering only a diffusion external radiation source, energy balance on the boundary gives the boundary conditions for the temperature as

$$K_c(T)\frac{\partial T}{\partial z}(0) = h[T(0) - T_{out}] - \pi\epsilon\sum_k [I_{bo}^{(k)}(T(0)) - I_{bo}^{(k)}(T_{out})], \tag{2.6}$$

$$-K_c(T)\frac{\partial T}{\partial z}(l) = h[T(l) - T_{out}] - \pi\epsilon\sum_k [I_{bo}^{(k)}(T(l)) - I_{bo}^{(k)}(T_{out})], \tag{2.7}$$

where h is the convection film coefficient, ϵ is the boundary emissivity in opaque spectral region, T_{out} is the surrounding temperature, K_c is the thermal conductivity of the material and $I_{bo}^{(k)}(T)$ is the blackbody radiation intensity with refractive index 1 for the spectral band k at temperature T.

3. **Numerical Method**

Here we develop a numerical method based on finite volume discretization to solve the nonlinear parabolic equation (2.4) with the boundary conditions (2.6)-(2.7) and initial condition $T(z, 0) = T_0(z)$, a specified function of position.

3.1. **Finite Volume Discretization.** We partition the region (the slab of length l) into N finite cells $Z_i = [z_{i-\frac{1}{2}}, z_{i+\frac{1}{2}}], i = 1, \cdots, N$ with length $\Delta z = l/N$ and define the nodes z_i as the midpoint of the cell Z_i.

$$z_{i-\frac{1}{2}} = i\Delta z,\ z_i = \tfrac{1}{2}(z_{i-\frac{1}{2}} + z_{i+\frac{1}{2}}),\ i = 1, \cdots, N$$

The boundaries are specified by

$$z_0 = z_{1-\frac{1}{2}} = 0,\ z_{N+1} = z_{N+\frac{1}{2}} = l.$$

Let $\Delta t = t_{max}/M$ be the time increments and define the discrete time-steps $t_j = j\Delta t$, $j = 0, 1, 2, \cdots, M$. The initial time is denoted by $j = 0$, the discrete approximations for T at the grid (z_i, t_j) is denoted by T_i^j. We also regard T_i^j as an approximation to mean value of $T(z, t)$ in the cell Z_i at time t_j.

If an approximate solution T_i^j is assumed to be known at all grid points at time t_j, a method must be specified to advance the solution to time t_{j+1}, subject to the boundary conditions.

Integrating equation (2.4) in the finite cell Z_i over the time interval $[t_j, t_{j+1}])$ we obtain

$$\int_{t_j}^{t_{j+1}} \int_{z_{i-\frac{1}{2}}}^{z_{i+\frac{1}{2}}} \left\{ \rho C(T) \frac{\partial T}{\partial t} - \frac{\partial}{\partial z} \left(K(T) \frac{\partial T}{\partial z} \right) \right\} dz\, dt = 0 \tag{3.1}$$

which implies

$$\int_{z_{i-\frac{1}{2}}}^{z_{i+\frac{1}{2}}} (T^{j+1} - T^j) dz \approx \frac{1}{\rho C(T)} \int_{t_j}^{t_{j+1}} \left(K(T) \frac{\partial T}{\partial z}(z_{i+\frac{1}{2}}, t) - K(T) \frac{\partial T}{\partial z}(z_{i-\frac{1}{2}}, t) \right) dt. \tag{3.2}$$

We assume that the time increment Δt is so brief that during the time $[t_j, t_{j+1}]$ the fluxes on the right hand side are constant and arbitrarily close to their values at any intermediate time interval. Let $t_{j+\theta} := t_j + \theta \Delta t = (1-\theta) t_j + \theta t_{j+1}$ to be some intermediate time with $0 \leq \theta \leq 1$. Then,

$$T_i^{j+1} = T_i^j + \frac{\Delta t}{\rho C(T_i^{j+\theta}) \Delta z} \left(F_{i-\frac{1}{2}}^{j+\theta} - F_{i+\frac{1}{2}}^{j+\theta} \right),\ i = 1, \cdots N,\ j = 0, \cdots, M \tag{3.3}$$

where

$$F_{i-\frac{1}{2}}^{j+\theta} = \frac{1}{2} \left(K(T_i^{j+\theta}) + K(T_{i-1}^{j+\theta}) \right) \left(\frac{T_i^{j+\theta} - T_{i-1}^{j+\theta}}{z_i - z_{i-1}} \right).$$

Here $\theta = 0$ and $\theta = 1$ yield the explicit and fully implicit schemes respectively.

The values at the boundary nodes z_0 and z_{N+1} are updated as follows.

$$T_0^{j+1} = \left(\alpha T_1^{j+1} + h T_{out} - \pi \epsilon \sum_k \left(I_{bo}^{(k)}(T_0^{j+\theta}) - I_{bo}^{(k)}(T_{out}) \right) \right) / (\alpha + h) \tag{3.4}$$

$$T_{N+1}^{j+1} = \left(\beta T_N^{j+1} + h T_{out} - \pi \epsilon \sum_k \left(I_{bo}^{(k)}(T_{N+1}^{j+\theta}) - I_{bo}^{(k)}(T_{out}) \right) \right) / (\beta + h) \tag{3.5}$$

where

$$\alpha = \frac{K_c(T_1^{j+\theta}) + K_c(T_0^{j+\theta})}{z_1 - z_0}, \quad \beta = \frac{K_c(T_{N+1}^{j+\theta}) + K_c(T_N^{j+\theta})}{z_{N+1} - z_N}.$$

For the above finite volume control formulation, there are $N+2$ equations for $N+2$ unknowns $T_0^{j+1}, T_1^{j+1}, ..., T_{N+1}^{j+1}$ for every time step Δt leading to a system of algebraic equations. For any implicit scheme ($\theta > 0$), the resulting system of equations (3.3) becomes nonlinear which needs to be solved by some iterative methods.

The fully implicit method is unconditionally stable. There is no restriction on the time step-size except for the accuracy. However the method involves iterative process, it is not desirable for many practical applications. The explicit method is easy to implement and very convenient for parallelization but it suffers from a severe stability restriction on the time step-size $\Delta t < \frac{1}{2} \left(\frac{\rho \min C(T)}{\max K(T)} \right) \Delta z^2$ known as Courant-Friedrichs-Lewy (CFL) condition.

3.2. **Super Time Stepping Schemes.** Using (3.3), (3.1), (3.4) and (3.5) we write the explicit scheme in the following matrix equation.

$$\mathbf{T}^{j+1} = R(\Delta t A)\mathbf{T}^j \tag{3.6}$$

Here $\mathbf{T}^j = \left[T_0^j, T_i^j, \cdots, T_n^j\right]^T$, $R = I - \Delta t A$ is the amplification factor, where A is the coefficient matrix that depends on T_i^j through $K(T)$ and $C(T)$.

The algorithm (3.6) is stable if the spectral radius of R is less than unity. The stability restriction (CFL condition) is equivalent to $\Delta t < \Delta t_{\text{expl}} := \frac{2}{\lambda_{\max}}$, where $\lambda_{\max}$ is the maximum eigenvalue of A.

Super time-stepping schemes relax restriction of the CFL condition by requiring stability at the end of a cycle of s time steps, rather than at the end of each time step Δt_{expl} , thus leading to a Runge-Kutta-like method with s stages. The intermediate steps are updated non–uniformly using some prespecified simple formula [1] or recurrence relation [5].

3.2.1. *Runge-Kutta Chebychev (RKC) scheme* [1]. In this scheme, a super-step $\Delta\tau$ is defined which is further subdivided into τ_k steps with $k = 1, 2, ..., s$ such that the duration of one super-step $\Delta\tau = \sum_{k=1}^{s} \tau_k$. The main idea of this scheme is to choose the intermediate steps τ_k which ensures stability at the end of the super-step $\Delta\tau$ and also maximize the duration of the super-step. Then the explicit scheme (3.6) can be expressed as

$$\mathbf{T}^{j+1} = R_s(\Delta\tau A)\mathbf{T}^j = \left(\prod_{k=1}^{s} (I - \tau_k\, A)\right)\mathbf{T}^j \tag{3.7}$$

where $\mathbf{T}^{j;l}$ denotes the computed temperature $\mathbf{T}$ at time $j\Delta\tau + \sum_{k=1}^{l} \tau_k$. Note that the stability requirement is

$$\rho\left(R_s(\Delta\tau A)\right)) < 1 \implies ||p_s(\lambda)|| < 1 \quad \forall\ \lambda \in [\lambda_{\min}, \lambda_{\max}] \tag{3.8}$$

where $p_s(\lambda) = \prod_{k=1}^{s} (1 - \tau_k\lambda)$ and λ are the eigenvalues of A. Using the properties of modified Chebyshev polynomial, the steps $\tau_1, \tau_2, \cdots, \tau_s$ are chosen subject to

$$|p_s(\lambda)| \le K,\ (0 < K < 1) \quad \text{and} \quad |p_s'(0)| = \sum_{k=1}^{s} \tau_k \quad \text{is maximal} \tag{3.9}$$

as

$$\tau_k = \Delta t_{\text{expl}} \left((-1+\nu)\cos\left(\frac{2k-1}{s}\frac{\pi}{2}\right) + 1 + \nu\right)^{-1}, \quad 0 < \nu < \frac{\lambda_{\min}}{\lambda_{\max}} \tag{3.10}$$

where ν is a damping coefficient. The upper bound on ν in (3.10) is only theoretical. In practice, we can use large ν (more accuracy, higher cost). Note that if the value

of ν is zero and $s = 1$, the explicit scheme is recovered. It can be shown that the resulting duration of the super-step

$$\Delta\tau = \sum_{k=1}^{s} \tau_k \to s^2\, \Delta t_{\text{expl}} \quad (\text{as } \nu \to 0). \tag{3.11}$$

Thus, s substeps of a superstep cover a time interval s times bigger than s explicit steps when $\nu \to 0$. The length of the superstep $\Delta\tau$ is determined by the choice of s and ν and is restricted only by accuracy just like in any unconditionally stable implicit methods.

3.2.2. *Runge-Kutta Legendre (RKL) scheme* [5]. Just like the Chebyshev polynomials, Legendre polynomials are also bounded in magnitude by unity and is useful to develop a stable scheme. As before, let $\Delta\tau$ be the duration of one superstep consisting of s intermediate steps. Instead of expressing stability polynomial in the factored form as in (3.7), this method defines R_s in terms of a Legendre polynomials.

$$R_s(z) = a_s + b_s P_s(w_0 + w_1 z) \tag{3.12}$$

The parameters $a_s = 0$, $b_s = 1$, $w_0 = 1$ and $w_1 = \frac{2}{s^2+s}$ are chosen to satisfy the consistency conditions at first order $R_s(0) = 1$ and $R_s'(0) = 1$. Thus, the s-stage RK scheme takes the form

$$\mathbf{T}^{j+1} = P_s\left(I - w_1 \Delta\tau A\right) \mathbf{T}^j \tag{3.13}$$

Using the three point recursion property of the Legendre polynomials

$$(k)P_k(x) = (2k-1)xP_{k-1}(x) - (k-1)P_{k-2}(x) \tag{3.14}$$

the RKL scheme (3.13) can be written as

$$\begin{cases} \mathbf{U}_0 = \mathbf{T}^j \\ \mathbf{U}_1 = \mathbf{U}_0 - \bar{\mu}_1 \Delta t A \mathbf{U}_0 \\ \mathbf{U}_k = \mu_k \mathbf{U}_{k-1} + \nu_k \mathbf{U}_{k-2} - \bar{\mu}_k \Delta t A \mathbf{U}_{k-1}, \quad 2 \le k \le s \\ \mathbf{T}^{j+1} = \mathbf{U}_s \end{cases} \tag{3.15}$$

where

$$\mu_k = \frac{2k-1}{k}, \quad \bar{\mu}_k = \frac{2k-1}{k} w_1, \quad \nu_k = \frac{1-k}{k}.$$

The maximum stable superstep for the above s-stage RKL scheme is given by

$$\Delta t_{\max} = \frac{\Delta t_{Expl}}{w_1} = \Delta t_{Expl} \frac{s^2 + s}{2}.$$

Note that unlike RKC, the RKL method described by the recursive relation (3.15) is consistent and stable at each of the intermediate stages which is more flexible for output.

4. **Numerical Computations**

The numerical procedure developed in the previous section is written in Fortran 90, compiled with Intel Fortran, and ran on Xeon-class processors (AMD Opteron 2378, 2400 MHz, 512 KB cache). Here we present some numerical simulations for a glass cooling problem with all the physical constants taken from [3]. The physical system consists of two infinite, parallel plates, between the plates there is a nongray medium (glass) which absorbs and emits radiation, but does not scatter. The glass has an initial temperature of $600°C$ uniformly distributed and start cooling down through radiation on the boundary surface which is directly exposed to the surrounding temperature of $T_{out} = 26.85°C$. The convection heat transfer coefficient h, the boundary emissivity ϵ, refractive index for the glass Rn_g, thermal conductivity K_c, specific heat capacity C and density of glass ρ all are taken to be constant throughout the computations as shown in the Table 1.

TABLE 1. Assumed constants for numerical computations

Parameter	Value	Description
Rn_g	1.46	Index of refraction for glass
K_T	1.03×10^5 erg-cm/s-K	Thermal Conductivity
C_T	0.98031×10^{10} erg-K/kg	Specific Heat Capacity
c_g	2.05342×10^{10} cm/s	Speed of light in glass
ϵ	0.89	Boundary Emissivity coefficient
ρ	2.22×10^{-3} kg/cm^{-3}	Density of glass
h	0.001	Convection film coefficient

Effect of convection in the total energy transport is found to be almost non-influencing. Absorption coefficient of glass $a(k)$ as a function of wave number for various spectral band widths is shown in the Table 2.

TABLE 2. Absorption coefficient for glass

η	1000-2000	2000-2500	2500-3500	3500-6000	6000-10000	10000-200000
$a(k)$	80.0	35.0	10.0	1.0	0.01	0.02

To compute blackbody radiation intensity in each spectral band, the following formula was employed.

$$I_b^k(T) = \int_{\eta_k}^{\eta_{k+1}} \frac{2c_1\eta^3}{\exp\left(\frac{c_2\eta}{T}\right) - 1} d\eta \tag{4.1}$$

where $c_1 = h_p c_0^2$ and $c_2 = h_p c_0 k_b^{-1}$. The integral is numerically computed using 6-point Gaussian quadrature (composite) rule [2]. A table of values of $I_b^{(k)}(T)$ and

$\frac{\partial I_b^{(k)}}{\partial T}$ for a wide range of temperature is generated and stored in a file. These values are then interpolated to compute the total conductivity $K(T)$ during the calculation. The blackbody radiation intensity $I_b^k(T)$ for different spectral bands as given by (4.1) and total conductivity coefficient $K(T)$ as given by equation (2.5) for the temperature $[280\text{K}, 2680\text{K}]$ are shown in Figure 1.

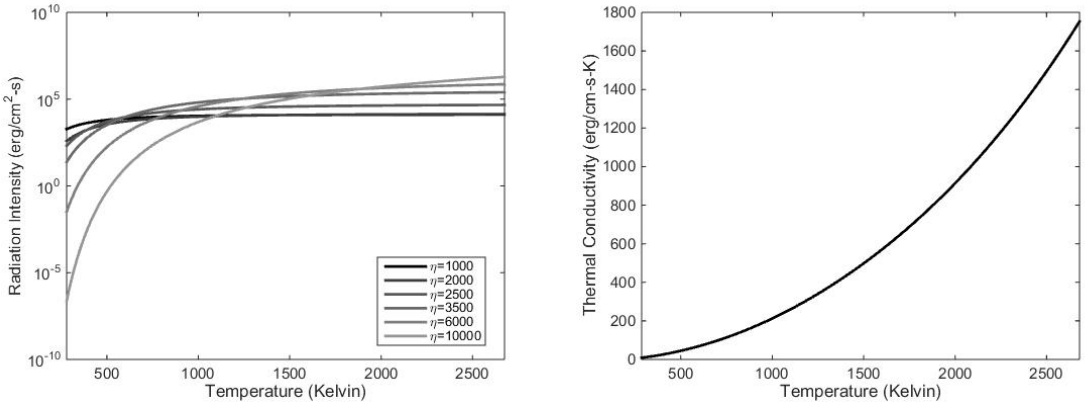

FIGURE 1. The blackbody radiation (left) and the conductivity (right)

To start simulation, we setup a fairly fine mesh of 200 control volumes with $\Delta z = 0.005$ cm and the time-step $\Delta t = 0.00001$ seconds satisfying the CFL condition. We present some simulation results up to $t_{\max} = 60$ seconds.

Temperature profiles at various times (t=1, 10, 30, 60s) obtained from pure conduction and the Rosseland approximation are shown in Figure 2. Here, by the pure conduction, we mean only the radiation term in the energy equation is neglected but the surface radiation given by the boundary conditions is taken into account. Solution of the energy equation without consideration of all the radiation effect, being constant, is of no interest.

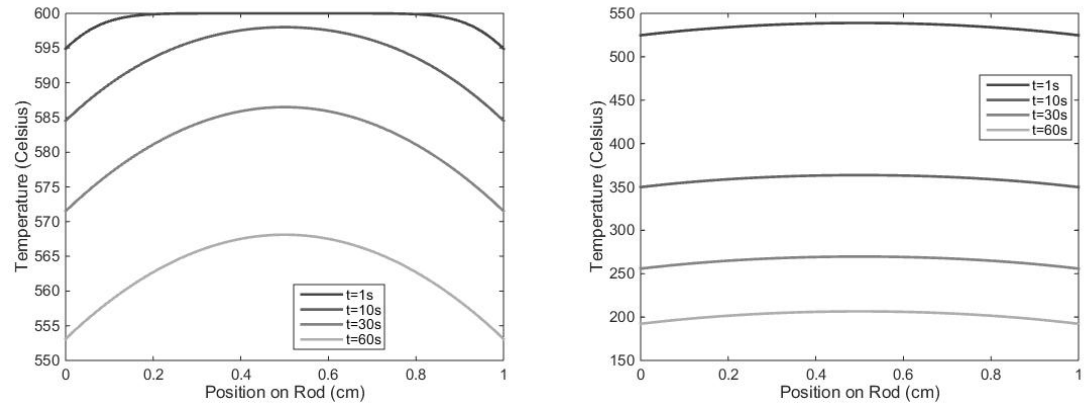

FIGURE 2. Temperature profile at various times using pure conduction (left), Rosseland approximation (right)

Figure 2 shows that the Rosseland approximation underestimates temperature profile whereas the pure conduction overestimates the same. It is natural to expect higher temperature profile from the pure conduction for the case of glass which has a very good infrared transmission property for which at temperatures higher than $400°C$ radiation is a major influencing component in the energy transport.

Next, we explored super time-stepping schemes to accelerate the explicit scheme. Since we do not have exact solution to estimate errors, we use the numerical solution reported earlier from the fully explicit scheme as the reference solution. First, we implemented the RKC method. Since this method has a damping parameter ν involved, we tried several runs with different combinations of the ν and s values. The solutions at the intermediate stages $< s$ are not outputted since they are not guaranteed to be stable as some of the values of τ_k will be greater than the Δt_{Expl}. Note that the larger the damping factor ν, the shorter the Δt becomes, improving the accuracy at the expense of more computations.

Speedup of the RKC super time-stepping scheme of stage s as well as their errors in L^2 and L^∞ norms are shown in the Table 3. The comparison is based on the explicit code, ($s = 1$, $\nu = 0$), which takes about 534 seconds for one simulation of $t_{\max} = 60$s. The errors displayed in the Table 3 show the increasing trend with the increase in the number of stages s. The same table also shows that the RKC scheme of a fixed stage s, the increasing values of ν reduces the error norms. The damping coefficient ν in RKC can be used as a "tune-up" parameter, trading speedup for accuracy.

We note that the RKC scheme (3.7) can be thought as a series of updates using forward Euler time-steps. The large value of ν that takes more computational time can be more accurate than the explicit Euler method.

Next, we experimented the other super time-stepping scheme namely RKL. The RKL scheme does not have the damping parameter ν and it needs some modification in the explicit Euler code. Looking at the algorithms (3.7) and (3.15), it seems that the RKL scheme is much more involved and it does require more function evaluations and memory storage. The numerical simulations show that for large values of s, RKL catches up with the speedup of the RKC scheme. The CPU timings as well as the errors resulting from different values of s are shown in the Table 4.

To compare the performance of the two super time-stepping schemes, we need to consider both accuracy and efficiency. RKC scheme has the advantage of having the damping parameter ν to monitor the errors and speedup. For the similar tuning in RKL, we introduce a parameter $\delta = \Delta t/\Delta t_{\max}$ and run the RKL code for several values of δ in $0 < \delta < 1$ to achieve speedup with an acceptable accuracy. The numerical results are presented in Table 5 and Figure 3.

TABLE 3. Test of RKC scheme in a simulation of $t_{\max} = 60$s.

s	ν	CPU Time (sec)	L^∞ - Error	L^2 - Error
1	0	533.67	–	–
2	0.0005	267.75	9.30400E-05	1.31826E-03
4	0.0005	134.61	4.32000E-04	6.12092E-03
4	0.0010	136.09	3.91741E-04	5.55054E-03
4	0.0050	146.94	4.00748E-04	5.67809E-03
4	0.0250	197.02	3.13941E-04	4.44805E-03
4	0.0500	251.31	1.88586E-04	2.67197E-03
4	0.1000	340.66	1.41799E-04	2.00902E-03
4	0.1250	378.88	4.00134E-05	5.66958E-04
4	0.2500	533.03	1.69318E-05	2.39894E-04
10	0.0005	56.82	3.09701E-03	4.38803E-02
10	0.0010	60.19	2.70092E-03	3.82683E-02
10	0.0050	84.82	1.50698E-03	2.13519E-02
10	0.0250	169.17	4.13328E-04	5.85634E-03
10	0.0500	238.46	3.68489E-04	5.22080E-03
10	0.1000	337.14	3.02805E-04	4.29007E-03
10	0.1250	379.51	5.56838E-05	7.88971E-04
10	0.2500	533.06	1.14577E-04	1.62327E-03
20	0.0005	33.47	5.64470E-03	7.99823E-02
20	0.0010	39.64	4.43230E-03	6.28032E-02
20	0.0050	76.06	2.92501E-03	4.14427E-02
20	0.0250	168.88	3.63746E-04	5.15390E-03
20	0.0500	238.82	1.42706E-04	2.02204E-03
20	0.1000	337.77	1.44767E-04	2.05107E-03
20	0.1250	377.61	1.21551E-04	1.72214E-03
20	0.2500	534.02	1.14656E-04	1.62439E-03
25	0.0005	29.49	7.07114E-03	1.00195E-01
25	0.0010	36.66	6.14839E-03	8.71177E-02
25	0.0050	75.39	2.53974E-03	3.59845E-02
25	0.0250	168.29	3.29416E-04	4.66753E-03
25	0.0500	238.00	5.06888E-04	7.18154E-03
25	0.1000	336.58	1.44771E-04	2.05114E-03
25	0.1250	376.32	3.50528E-04	4.96616E-03
25	0.2500	532.19	2.76567E-04	3.91826E-03
25	0.5000	753.27	2.40535E-05	3.40761E-04
50	0.0050	75.75	1.54492E-03	2.18904E-02

TABLE 4. Test of RKL scheme in a simulation for $t_{\max} = 60$s.

s	δ	CPU Time (sec)	L^∞ - Error	L^2 - Error
1	1.00	533.67	–	–
2	0.90	357.44	1.86496E-02	2.57524E-01
4	0.90	214.50	1.15669E-02	1.59531E-01
6	0.90	152.69	6.82398E-03	9.39144E-02
8	0.90	119.11	4.08382E-03	5.59487E-02
10	0.90	97.21	2.71804E-03	3.71062E-02
12	0.90	82.38	6.41650E-04	8.02056E-03
16	0.90	63.08	7.30341E-04	1.00551E-02
20	0.90	50.99	2.15566E-03	3.04428E-02
25	0.90	41.33	7.40035E-03	1.05113E-01
50	0.90	21.12	3.76210E-02	5.33117E-01

TABLE 5. Test of RKL scheme with $\Delta t/\Delta t_{Expl} = \delta(\frac{s^2+s}{2})$ and $0 < \delta < 1$.

s	δ	CPU Time (sec)	L^∞ - Error	L^2 - Error
1	1	533.67	–	–
25	0.9000	41.30	7.40035E-03	1.05113E-01
25	0.8000	46.47	5.26300E-03	7.47614E-02
25	0.7000	53.10	3.12282E-03	4.43216E-02
25	0.6000	61.96	4.48381E-03	6.36895E-02
25	0.5000	74.34	3.50634E-03	4.98065E-02
25	0.4000	92.93	3.70110E-03	5.25590E-02
25	0.3000	123.90	1.56289E-03	2.21917E-02
25	0.2000	185.86	1.75300E-03	2.48974E-02
25	0.1000	371.71	7.79211E-04	1.10680E-02
25	0.0500	743.42	2.92405E-04	4.15314E-03
50	0.9000	21.08	3.76210E-02	5.33117E-01
50	0.4500	42.15	1.87330E-02	2.65460E-01
50	0.2250	84.32	9.28969E-03	1.31642E-01
50	0.1125	168.67	4.56815E-03	6.47344E-02

RKC is more accurate for $s \leq 15$ but RKL seems to be more consistent in error also for larger s. RKC with appropriately chosen ν always performs better than RKL for the same s. RKC with $\nu = 0.0005$ is found to have the best performance both in speedup as well as accuracy.

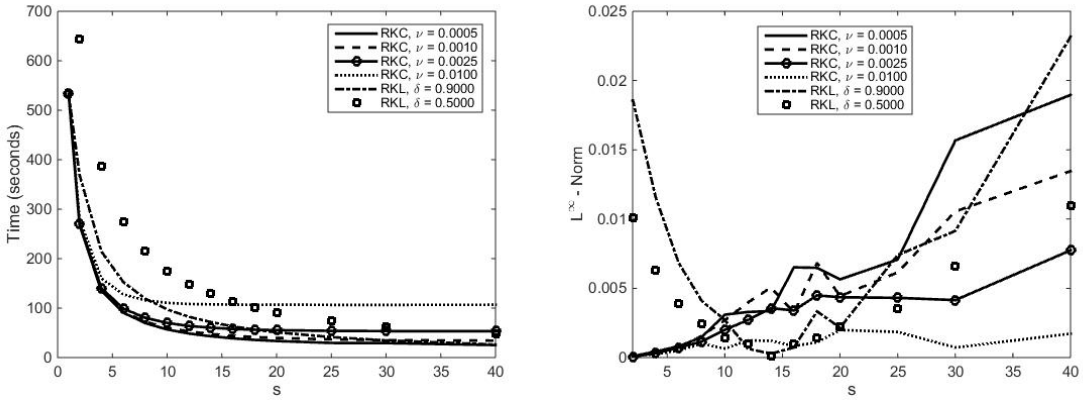

FIGURE 3. Test comparison of the two super time-stepping schemes speedup (left) and error (right).

5. **Conclusion**

In this paper, we considered a nonlinear parabolic partial differential equation modeling a coupled conduction and radiation heat transfer problem and solved it numerically using explicit finite volume method with super time-stepping strategy. We implemented two first order super time-stepping schemes (RKC and RKL) and found that both the methods work well for the model problem and boast large efficiency gains compared to standard explicit Euler method. Based on the numerical simulations, we confirmed that the RKC performed better than the RKL in the speedup providing we can choose the damping parameter (ν) appropriately by trial and error. Tuning in the RKL scheme can be done by reducing the time-step size $\Delta t < \Delta t_{\max}$. Both the super time-stepping methods can be easily implemented and parallelized for problems in higher dimensions and with intricate geometry.

REFERENCES

[1] V. Alexiades, V. Amiez, P.-A., Gremaud, "Super-Time-Stepping acceleration of explicit schemes for parabolic problems", Communications in Numerical Methods in Engineering, 12, 31-42, 1996.

[2] Ward Cheney, David Kincaid, *Numerical Mathematics and Computing, 7th ed.*, Brooks/Cole Publishing Company, 2013.

[3] Khanal, H., Uprety, K.N., "Diffusion Approximation to Radiation Heat Transfer in Semitransparent Medium", *The Nepali Math. Sc. Report*, Vol. 34, No. 1 & 2, pp. 25-38, 2016.

[4] Chad D. Meyer, Dinshaw S. Balsara, Tariq D. Aslam, "A stabilized Runge-Kutta-Legendre method for explicit super-time-stepping of paraboliic and mixed equations", *Journal of Computational Physics*, 257, 594-626, 2014.

[5] M.F. Modest, *Radiation Heat Transfer*. Academic Press, 2003.

[6] J.W. Thomas, *Numerical Partial Differential Equations: Finite Difference Methods*, Text in Applied Mathematics, Springer, 2010.